

Transport through a quantum spin Hall quantum dot

Carsten Timm*

Institute of Theoretical Physics, Technische Universität Dresden, 01062 Dresden, Germany

(Received 14 November 2011; revised manuscript received 17 September 2012; published 31 October 2012)

Quantum spin Hall insulators, recently realized in HgTe/(Hg,Cd)Te quantum wells, support topologically protected, linearly dispersing edge states with spin-momentum locking. A local magnetic exchange field can open a gap for the edge states. A quantum-dot structure consisting of two such magnetic tunneling barriers is proposed, and the charge transport through this device is analyzed. The effects of the bias voltage, the gate voltage, and the charging energy in the quantum dot are studied employing Landauer and master-equation approaches. For vanishing charging energy, the differential conductance is periodic in both gate and bias voltages. For nonzero charging energy, the periodicity in the gate voltage is retained, but with increased period. A partial recurrence of the noninteracting periodicities is found for strong interactions. The possibility of controlling the edge magnetization by a locally applied gate voltage is proposed.

DOI: [10.1103/PhysRevB.86.155456](https://doi.org/10.1103/PhysRevB.86.155456)

PACS number(s): 73.23.-b, 03.65.Vf, 05.60.Gg, 71.10.Pm

I. INTRODUCTION

Topological insulators and superconductors^{1–3} have recently become the topic of extensive experimental and theoretical research. These materials can be described in terms of weakly interacting quasiparticles with Hamiltonians showing nontrivial topological properties in momentum space. They have an energy gap in the bulk but a topologically protected gapless spectrum of boundary states. Schnyder *et al.*^{2,4} and Kitaev⁵ have put forward an exhaustive classification of these systems in terms of their Altland-Zirnbauer symmetry classes⁶ and of the number of spatial dimensions.

A topologically nontrivial state is possible for the symplectic class AII in two dimensions, corresponding to systems with spin-orbit coupling in the absence of an applied magnetic field and of superconductivity. This so-called quantum spin Hall (QSH) state^{7,8} has protected edge states with gapless Weyl-type dispersion. Bernevig *et al.*⁹ have predicted and König *et al.*^{10,11} have observed the QSH state in HgTe/(Hg,Cd)Te quantum wells.

The edge states of the QSH system show spin-momentum locking in the sense that right-moving (left-moving) electrons are strictly spin up (spin down).^{1,3,11} Consequently, density-density interactions cannot lead to backscattering since they cannot flip the spin. On the other hand, spin-dependent scattering, for example by magnetic impurities, can lead to backscattering. Unconventional transport properties are thus expected, and possible applications in spintronics can be envisaged. It is therefore of interest to study electronic transport in prototypical device geometries involving QSH edge states.

The idea at the basis of this paper is to realize a quantum dot as a finite-length segment of a QSH edge. This cannot be achieved by electrostatic gating since an electric potential just shifts the edge bands without opening a gap and thus does not lead to the formation of tunneling barriers. However, such barriers could be realized by ferromagnetic insulators imposing a magnetic exchange field orthogonal to the spin-orbit field and opening a gap. We here consider parallel and antiparallel exchange fields in the two barriers and assume the barriers to be thin. We also include a gate electrode that can be used to tune the electrostatic potential on the quantum dot.

Figure 1 shows a sketch of the device. Finally, we assume the thermal energy $k_B T$ to be small compared to the lifetime broadening of the dot levels so that we can set the temperature to zero. Including a finite temperature is straightforward. An alternative realization of a QSH quantum dot as the edge of a small QSH puddle has been analyzed by Tkachov and Hankiewicz,¹² assuming negligible charging energy.

After introducing the model in Sec. II, we study the effect of the gate and bias voltages on the transport in Sec. III. A Landauer approach¹³ is used to obtain the current for arbitrary strength of the magnetic barriers. The effect of the electron-electron interaction within the dot is studied in Sec. IV. We employ a simple model including a charging energy in terms of the excess charge. This is valid if the range of the electron-electron interaction is large compared to the dot size W but should give qualitatively correct results beyond this regime. The opposite case of short-range interactions has been studied for an unmodulated QSH edge in Refs. 14–16. A quantum dot in a spinless Luttinger liquid, not a QSH edge, has been studied by several authors.^{17–20} Tunneling through a quantum dot between two QSH edges has been addressed by Law *et al.*²¹

II. MODEL

The noninteracting part of the Hamiltonian of the QSH edge with magnetic barriers is written as a 2×2 matrix in spin space,

$$H_0 = -i\hbar v_F \sigma^z \partial_x - \eta \hbar v_F \sigma^x \delta(x) \mp \eta \hbar v_F \sigma^x \delta(x - W) + V(x), \quad (1)$$

where v_F is the Fermi velocity, σ^x and σ^z are Pauli matrices, η is the dimensionless strength of the magnetic barriers, and $V(x)$ is a nonuniform electric potential. A 2×2 unit matrix is implied in the last term. H_0 is only valid within the bulk energy gap. The first term is the Weyl Hamiltonian of the bare edge.^{11,22} We neglect higher-order spatial derivatives, which lead to nonlinear terms in the dispersion. An electric field perpendicular to the layers would induce an additional Rashba spin-orbit-coupling term $H_R = -i\alpha \sigma^y \partial_x$. However, this term can be absorbed into the Weyl term by a rotation in spin space.²² The upper (lower) sign of the third term refers to

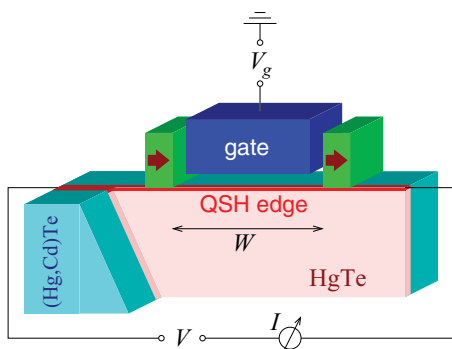


FIG. 1. (Color online) Cutaway view of the QSH quantum dot.

parallel (antiparallel) exchange fields in the two barriers. The parameter η can be written as

$$\eta = \frac{g\mu_B B_{\text{exc}} L}{\hbar v_F}, \quad (2)$$

where g is the g factor, μ_B is the Bohr magneton, B_{exc} is the exchange field, and L is the length of the magnetic barrier. Equation (1) is obtained in the limit of thin barriers, $L \rightarrow 0$, $B_{\text{exc}} \rightarrow \infty$, $B_{\text{exc}} L = \text{const}$. This limit is valid if $|E - V(x)| \ll g\mu_B B_{\text{exc}}$ since then the potential term proportional to $E - V(x)$ is negligible compared to the field term in the barrier. In this case, the transfer matrices of the barriers, introduced below, only depend on $\eta \propto B_{\text{exc}} L$. Exchange energies on the order of several tens of meV appear to be feasible. Then the bias and gate voltages should be limited to a few millivolts. This does not impose an additional constraint, however, since the maximum bulk gap of HgTe/(Hg,Cd)Te wells in the QSH regime is calculated¹⁰ as $E_g = 40$ meV and our approach is only applicable within the gap in any case.

The limit is also valid for $|E - V(x)| L / \hbar v_F \ll 1$ since then the phase accumulated by an electron traveling through the barrier due to the potential term is negligible. Teo and Kane²³ give $\hbar v_F = 0.35$ eV nm. Taking a typical value of $|E - V(x)| = 10$ meV (see previous point), we obtain $L \ll \hbar v_F / |E - V(x)| = 35$ nm. Thus the limit is also valid for very thin barriers for any B_{exc} . For $V(x)$ we take

$$V(x) = \begin{cases} eV/2 & \text{for } x \leq 0, \\ -eV_g & \text{for } 0 < x \leq W, \\ -eV/2 & \text{for } x > W, \end{cases} \quad (3)$$

where V is the bias voltage and V_g is the gate voltage.

Multiplying the time-independent Schrödinger equation resulting from H_0 by σ^z from the left, we obtain

$$\begin{aligned} \partial_x \psi &= i \frac{E - V(x)}{\hbar v_F} \sigma^z \psi(x) \\ &- \eta \sigma^y \delta(x) \psi(x) \mp \eta \sigma^y \delta(x - W) \psi(x), \end{aligned} \quad (4)$$

which for $x \geq x_0$ is solved by means of a (nonunitary) ‘‘spatial-evolution operator,’’

$$\begin{aligned} \psi(x) &= S_{\leftarrow} \exp \left\{ \int_{x_0}^x dx' \left[i \frac{E - V(x')}{\hbar v_F} \sigma^z \right. \right. \\ &\left. \left. - \eta \sigma^y \delta(x') \mp \eta \sigma^y \delta(x' - W) \right] \right\} \psi(x_0), \end{aligned} \quad (5)$$

where S_{\leftarrow} is a spatial-ordering directive; operators acting on $\psi(x_0)$ are ordered with their spatial coordinates increasing from right to left. Equation (5) implies the boundary condition

$$\psi(0^+) = e^{-\eta \sigma^y} \psi(0^-) = (\cosh \eta - \sigma^y \sinh \eta) \psi(0^-) \quad (6)$$

at the barrier at $x = 0$. Since the Schrödinger equation is of first order, there is only a single boundary condition. Analogously, we find $\psi(W^+) = (\cosh \eta \mp \sigma^y \sinh \eta) \psi(W^-)$.

In the following, we will need the eigenstates of the decoupled dot, i.e., for $\eta \rightarrow \infty$. The Schrödinger equation for the eigenspinors $\psi_\nu(x)$ to eigenenergies E_ν reads

$$-i\hbar v_F \sigma^z \partial_x \psi_\nu - eV_g \psi_\nu(x) = E_\nu \psi_\nu(x), \quad (7)$$

with the boundary conditions

$$(1 + \sigma^y) \psi_\nu(0) = 0, \quad (1 \mp \sigma^y) \psi_\nu(W) = 0. \quad (8)$$

The normalized solutions are

$$\psi_\nu(x) = \frac{1}{\sqrt{2W}} \begin{pmatrix} \exp\left(i \frac{E_\nu + eV_g}{\hbar v_F} x\right) \\ -i \exp\left(-i \frac{E_\nu + eV_g}{\hbar v_F} x\right) \end{pmatrix}, \quad (9)$$

with

$$\begin{aligned} E_\nu &= -eV_g + \frac{\pi \hbar v_F}{W} \\ &\times \begin{cases} \nu + 1/2 & \text{for parallel exchange fields,} \\ \nu & \text{for antiparallel exchange fields,} \end{cases} \end{aligned} \quad (10)$$

where ν can assume any integer value. Note that the spectrum is an equidistant ladder of nondegenerate levels. The level spacing is $E_0 := \pi \hbar v_F / W$. Of course, the discrete spectrum only exists inside the bulk gap and is only equidistant as long as nonlinear terms in the dispersion can be neglected. For vanishing voltages, $V = V_g = 0$, the spectrum is symmetric with respect to zero energy for both orientations of the exchange fields due to the particle-hole symmetry of H_0 . For antiparallel exchange fields, one eigenstate has energy zero, whereas for parallel exchange fields all eigenenergies come in pairs of opposite sign. Since the particle-hole symmetry is only approximate in a real device, this symmetry of the spectrum is only approximate as well.

Finally the charging energy is described by the particle-hole-symmetric term,

$$H_{\text{int}} = \frac{e^2}{2C} \left[\sum_\nu \left(n_\nu - \frac{1}{2} \right) \right]^2, \quad (11)$$

where C is the capacitance of the quantum dot and $n_\nu = c_\nu^\dagger c_\nu$ is the number operator of the single-particle state $|\nu\rangle$. $\sum_\nu (n_\nu - 1/2)$ denotes the *excess charge*.

III. TRANSPORT THROUGH A NONINTERACTING DOT

To study transport, we assume the states in both leads to be filled up to the chemical potential μ , measured relative to the Weyl nodes, which are shifted by the potential $\pm eV/2$. Neglecting the electron-electron interaction, the current through the QSH quantum dot can be expressed in terms of its transmission coefficient $T(E)$ by the Landauer formula,¹³

$$I = \frac{e}{h} \int_{\mu - eV/2}^{\mu + eV/2} dE T(E). \quad (12)$$

Since $T(E)$ does not depend on the bias voltage V in our case, the differential conductance is simply given by

$$\frac{dI}{dV} = \frac{e^2}{h} \frac{T(\mu + eV/2) + T(\mu - eV/2)}{2}. \quad (13)$$

The transmission coefficient $T(E)$ is obtained from the transfer matrix $\mathcal{T} = \mathcal{T}_R \mathcal{T}_{\text{dot}} \mathcal{T}_L$ of the device, where the three factors are the transfer matrices of the right barrier, the dot region, and the left barrier, respectively. Since the right-moving (left-moving) electrons have spin up (down), Eq. (6) implies

$$\mathcal{T}_L = \cosh \eta - \sigma^y \sinh \eta = \begin{pmatrix} \cosh \eta & i \sinh \eta \\ -i \sinh \eta & \cosh \eta \end{pmatrix}. \quad (14)$$

For the right barrier we get

$$\mathcal{T}_R = \begin{pmatrix} \cosh \eta & \pm i \sinh \eta \\ \mp i \sinh \eta & \cosh \eta \end{pmatrix}. \quad (15)$$

The transfer matrix for the dot region can be inferred from Eq. (5) for $x_0 = 0^+$, $x = W^-$,

$$\mathcal{T}_{\text{dot}} = \exp \left(i \frac{E + eV_g}{\hbar v_F} \sigma^z W \right). \quad (16)$$

The transmission coefficient $T = |t|^2$ obtained from $\mathcal{T}_R \mathcal{T}_{\text{dot}} \mathcal{T}_L \begin{pmatrix} 1 \\ r \end{pmatrix} = \begin{pmatrix} 1 \\ 0 \end{pmatrix}$ reads

$$T(E) = \frac{1}{1 + \text{trg}^2 \left(\frac{E + eV_g}{\hbar v_F} W \right) \sinh^2 2\eta}, \quad (17)$$

where $\text{trg} = \cos$ (\sin) for parallel (antiparallel) exchange fields. The transmission reaches unity whenever E matches an eigenenergy E_v of the decoupled dot. The width of the maxima is controlled by the barrier strength η . This is more easily seen by rewriting $T(E)$ as

$$T(E) = \frac{E_0}{2\pi \cosh 2\eta} \sum_{v=-\infty}^{\infty} \frac{2\gamma}{(E - E_v)^2 + \gamma^2}, \quad (18)$$

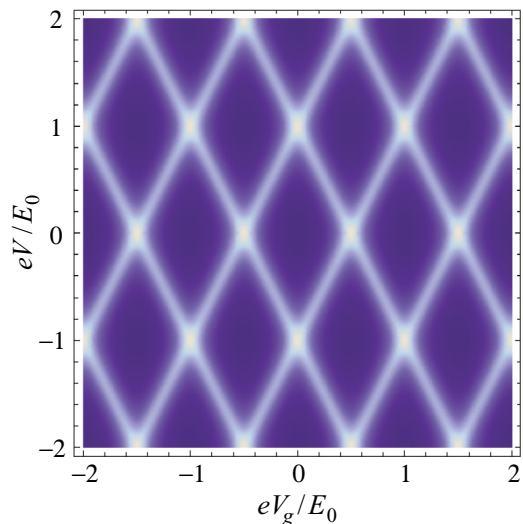
where the width of the Lorentzian peaks is

$$\gamma := \frac{E_0}{\pi} \ln \coth \eta = \frac{\hbar v_F}{W} \ln \coth \eta. \quad (19)$$

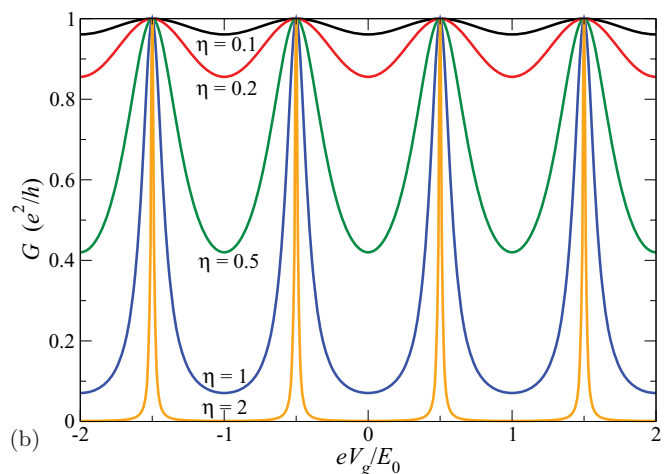
An analytical expression for the current can be obtained by inserting $T(E)$ into Eq. (12):

$$I = \frac{e}{h} \frac{\hbar v_F}{W \cosh 2\eta} \sum_v \left(\arctan \frac{E_v - \mu + \frac{eV}{2}}{\gamma} - \arctan \frac{E_v - \mu - \frac{eV}{2}}{\gamma} \right). \quad (20)$$

The differential conductance dI/dV can be read off from Eqs. (13) and (17). Since the chemical potential μ and the gate voltage V_g only appear in the combination $eV_g + \mu$, we can set $\mu = 0$ without loss of generality. dI/dV is plotted in Fig. 2(a) as a function of gate and bias voltages. Figure 2(a) clearly exhibits the suppression of the low-bias conductance off resonance due to Pauli blockade. As Fig. 2(b) shows, the resonant conduction maxima are broadened for strong coupling to the leads (weak magnetic barriers), and for $\eta \rightarrow 0$ we recover the constant conductance $dI/dV = e^2/h$ of an open channel. dI/dV is periodic in the gate voltage with period $E_0 = \pi \hbar v_F / W$ and in the bias voltage with period



(a)



(b)

FIG. 2. (Color online) (a) Differential conductance dI/dV through a QSH quantum dot for the strength $\eta = 1$ of the magnetic barriers and parallel exchange fields as a function of gate voltage V_g and bias voltage V in the absence of electron-electron interaction. Light colors denote large dI/dV . (b) Linear conductance $G = dI/dV|_{V=0}$ as a function of the gate voltage V_g . The level spacing of the decoupled dot, $E_0 = \pi \hbar v_F / W$, is used as the energy unit.

$2E_0$. Also, going from parallel to antiparallel exchange fields has the same effect as shifting eV_g by half a period, $E_0/2$. Furthermore, dI/dV is symmetric under reversal of the gate voltage V_g for both parallel and (not shown) antiparallel exchange fields. These symmetries are present to the extent that the approximations of linear dispersion and of particle-hole symmetry are satisfied.

IV. TRANSPORT THROUGH AN INTERACTING DOT

In this section we consider the effect of the charging energy H_{int} given by Eq. (11). Since H_{int} preserves particle-hole symmetry, the current is still odd, and dI/dV is even in the bias voltage. Beyond that, an exact solution does not exist. Here, we consider the case of weak coupling to the leads (strong magnetic barriers) but arbitrary interaction strength. A Pauli master equation, i.e., a master equation for the diagonal components of the reduced density operator of the quantum

dot, is well suited for this limit.^{24–26} It is then reasonable to retain only the terms of leading order in the coupling, which constitutes the sequential-tunneling approximation. Strictly speaking, the broadening of dot states due to the coupling should be neglected in this approximation. However, then the noninteracting limit would not be recovered correctly. Therefore, we include the broadening beyond sequential tunneling.^{27–29}

Let us denote the many-particle states of the dot in the occupation-number basis by $\vec{m} := |\dots, m_0, m_1, \dots\rangle$, where $m_\nu = 0, 1$ is the occupation number of single-particle state $|\nu\rangle$. Then the probabilities $P(\vec{m})$ of these states satisfy the Pauli master equation

$$\frac{d}{dt} P(\vec{m}) = \sum_{\vec{m}'} [R_{\vec{m}' \rightarrow \vec{m}} P(\vec{m}') - R_{\vec{m} \rightarrow \vec{m}'} P(\vec{m})]. \quad (21)$$

Here, $R_{\vec{m} \rightarrow \vec{m}'}$ is the transition rate from state \vec{m} to state \vec{m}' . For the stationary solution, the time derivative vanishes. In practice, the Fock space of the dot is truncated by restricting the single-particle basis to a sufficient number of states. For sequential tunneling, the rates $R_{\vec{m} \rightarrow \vec{m}'}$ vanish unless \vec{m} and \vec{m}' differ in exactly one of the occupation numbers m_μ . If $|\nu\rangle$ is the corresponding single-particle state, the rates are

$$\begin{aligned} R_{\vec{m} \rightarrow \vec{m}'} &= R_{\vec{m}, \nu}^{\text{in}} := R_0 \left(\int_{-\infty}^{\mu - eV/2} + \int_{-\infty}^{\mu + eV/2} \right) \frac{dE}{2\pi} \\ &\times \frac{2\gamma}{\left[E - E_\nu - \frac{e^2}{C} \sum_{\mu \neq \nu} (m_\mu - \frac{1}{2}) \right]^2 + \gamma^2} \\ &= \frac{R_0}{\pi} \left[\pi - \arctan \frac{E_\nu + \frac{e^2}{C} \sum_{\mu \neq \nu} (m_\mu - \frac{1}{2}) - \mu + \frac{eV}{2}}{\gamma} \right. \\ &\quad \left. - \arctan \frac{E_\nu + \frac{e^2}{C} \sum_{\mu \neq \nu} (m_\mu - \frac{1}{2}) - \mu - \frac{eV}{2}}{\gamma} \right] \end{aligned} \quad (22)$$

for $m_\nu = 0$ and $m'_\nu = 1$, and

$$\begin{aligned} R_{\vec{m} \rightarrow \vec{m}'} &= R_{\vec{m}, \nu}^{\text{out}} := R_0 \left(\int_{\mu - eV/2}^{\infty} + \int_{\mu + eV/2}^{\infty} \right) \frac{dE}{2\pi} \\ &\times \frac{2\gamma}{\left[E - E_\nu - \frac{e^2}{C} \sum_{\mu \neq \nu} (m_\mu - \frac{1}{2}) \right]^2 + \gamma^2} \\ &= \frac{R_0}{\pi} \left[\pi + \arctan \frac{E_\nu + \frac{e^2}{C} \sum_{\mu \neq \nu} (m_\mu - \frac{1}{2}) - \mu + \frac{eV}{2}}{\gamma} \right. \\ &\quad \left. + \arctan \frac{E_\nu + \frac{e^2}{C} \sum_{\mu \neq \nu} (m_\mu - \frac{1}{2}) - \mu - \frac{eV}{2}}{\gamma} \right] \end{aligned} \quad (23)$$

for $m_\nu = 1$ and $m'_\nu = 0$, respectively. R_0 is a characteristic rate further discussed below. The rate for tunneling into (out of) state $|\nu\rangle$, $R_{\vec{m}, \nu}^{\text{in}}$ ($R_{\vec{m}, \nu}^{\text{out}}$), is proportional to the spectral weight of this state below (above) the electrochemical potentials in the leads. The central energy of the dot states $|\nu\rangle$ for given occupation numbers m_μ , $\mu \neq \nu$, of the other states is shifted by the interaction energy $e^2/C \sum_{\mu \neq \nu} (m_\mu - 1/2)$. Furthermore, it is assumed that the level broadening due to the coupling to the leads is not affected by the interaction within the dot.

The current through lead α reads^{24,30,31}

$$I^\alpha = -\alpha \frac{e}{\hbar} \sum_{\vec{m}, \vec{m}'} \left(\sum_\nu m'_\nu - \sum_\nu m_\nu \right) R_{\vec{m} \rightarrow \vec{m}'}^\alpha P(\vec{m}), \quad (24)$$

where $\alpha = L = 1$ ($\alpha = R = -1$) for the left (right) lead. $R_{\vec{m} \rightarrow \vec{m}'}^\alpha$ denotes the part of the rates in Eqs. (22) and (23) due to lead α . The symmetrized current is

$$\begin{aligned} I &= \frac{I^L + I^R}{2} = -\frac{e}{2\hbar} \sum_{\vec{m}} \sum_\nu \\ &\times \left\{ \begin{array}{ll} R_{\vec{m}, \nu}^{L, \text{in}} - R_{\vec{m}, \nu}^{R, \text{in}} & \text{for } m_\nu = 0 \\ -R_{\vec{m}, \nu}^{L, \text{out}} + R_{\vec{m}, \nu}^{R, \text{out}} & \text{for } m_\nu = 1 \end{array} \right\} P(\vec{m}). \end{aligned} \quad (25)$$

We assume that the characteristic rate R_0 is not affected by interactions within the dot. Then R_0 has to be chosen in such a way that Eq. (20) is recovered for $e^2/C \rightarrow 0$. Inserting the rates into Eq. (25), we find $R_0 = \hbar v_F / (W \cosh 2\eta)$. The current is then

$$\begin{aligned} I &= \frac{e}{\hbar} \frac{\hbar v_F}{W} \frac{1}{\cosh 2\eta} \sum_{\vec{m}} \sum_\nu P(\vec{m}) \\ &\times \left[\arctan \frac{E_\nu + \frac{e^2}{C} \sum_{\mu \neq \nu} (m_\mu - \frac{1}{2}) - \mu + \frac{eV}{2}}{\gamma} \right. \\ &\quad \left. - \arctan \frac{E_\nu + \frac{e^2}{C} \sum_{\mu \neq \nu} (m_\mu - \frac{1}{2}) - \mu - \frac{eV}{2}}{\gamma} \right]. \end{aligned} \quad (26)$$

Chemical potential and gate voltage only appear as $eV_g + \mu$ in Eqs. (22), (23), and (26) so that the current only depends on this combination, as in the noninteracting case. We thus set $\mu = 0$ without loss of generality. The current is then still odd in the bias voltage and even in the gate voltage. The current remains periodic in eV_g , but the period is changed to $E_0 + e^2/C$ since a shift of eV_g by $E_0 + e^2/C$ in Eqs. (22), (23), and (26) can be compensated for by shifting the ladder of single-particle states by one level spacing E_0 , taking into account that this will also increase or decrease the excess charge in the stationary state by one unit. Moreover, the change from parallel to antiparallel exchange fields is equivalent to a shift of eV_g by half that period. For antiparallel exchange fields and $\mu = eV_g = 0$, a conductance peak remains pinned at zero bias due to particle-hole symmetry.

Note that our approach not only is valid for weak coupling to the leads but also recovers the exact results in the limit of weak interactions for any coupling. Moreover, the limit of *strong* coupling to the leads ($\eta \rightarrow 0$, $\gamma \rightarrow \infty$) is also correct: The current then approaches $I = (e^2/h)V$, the result for an open channel, for any interaction strength.

Figure 3 shows the differential conductance dI/dV for various interaction strengths e^2/C and otherwise the same parameters as in Fig. 2(a). With increasing e^2/C , the Pauli-blockade diamonds morph into Coulomb-blockade diamonds and become larger, in agreement with the gate-voltage period $E_0 + e^2/C$. Compared to the noninteracting case, the conductance peaks are split since the energy of the dot single-particle states now depends on the occupation of all other states. The peaks demarcating the Coulomb diamonds are particularly strong. Weak conductance peaks are visible

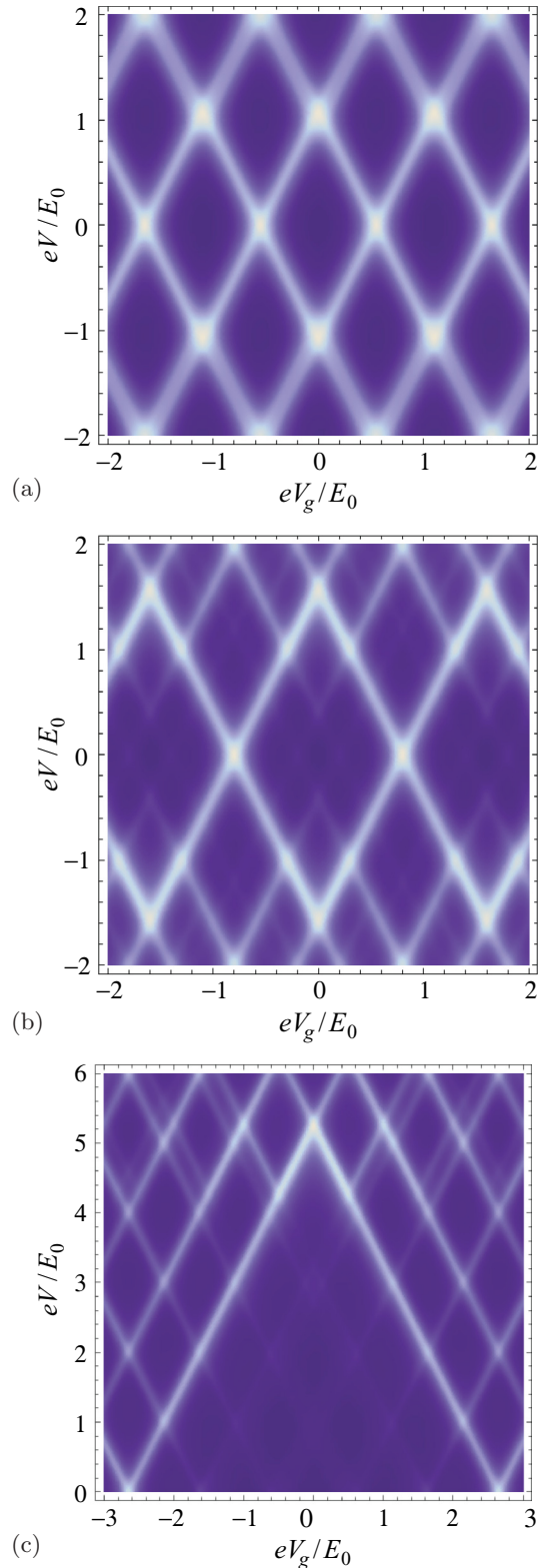


FIG. 3. (Color online) Differential conductance dI/dV through a QSH quantum dot with parallel exchange fields as a function of gate voltage V_g and bias voltage V . The dimensionless strength of the magnetic barriers is $\eta = 1$ ($\gamma = 0.086689 E_0$). The interaction strength is (a) $e^2/C = 0.1 E_0$, (b) $e^2/C = 0.6 E_0$, and (c) $e^2/C = 4.3 E_0$.

inside the Coulomb diamonds. While a single dot charge dominates in this regime, other dot charges have nonzero probabilities controlled by the tails of the Lorentzian peaks, which fall off like power laws in the energy distance from the Coulomb-blockade threshold. These subdominant dot charges lead to satellite peaks in dI/dV , which are stronger than those obtained from standard sequential-tunneling calculations without broadening but at nonzero temperature. In that case the peaks are *exponentially* suppressed by the tail of the Fermi distribution function. It should be emphasized that broadening effects first emerge at order R_0^2 and that at the same order additional effects, namely, cotunneling and pair tunneling, occur, which are not included here.²⁵

In the case of strong interactions [Fig. 3(c)], the sequential-tunneling lines show an approximate periodicity with the *noninteracting* periods E_0 in eV_g and $2E_0$ in eV . The explanation is that lines separated by E_0 in the gate voltage result from *different* single-particle states $|v\rangle$ and $|v+1\rangle$ but with the *same* occupation number of the other states. The interaction strength e^2/C then drops out of the energy difference.

We finally turn to the consequences of spin-momentum locking. From the continuity equation for the one-dimensional charge and current densities, $\partial_t \rho + \partial_x j = 0$, one easily obtains the charge current in terms of the many-particle wave function Ψ ,

$$j(x) = -ev_F \int dx_1 dx_2 \cdots \sum_{\sigma_1, \sigma_2, \dots = \pm 1} \sum_i \delta(x - x_i) \times \Psi_{\sigma_1 \sigma_2 \dots}^*(x_1, x_2, \dots) \sigma_i \Psi_{\sigma_1 \sigma_2 \dots}(x_1, x_2, \dots). \quad (27)$$

This expression is proportional to the z component of the one-dimensional spin density ρ^z ,

$$j(x) = -\frac{2ev_F}{\hbar} \rho^z(x). \quad (28)$$

In the stationary state, the current $j(x) = I$ is uniform so that the z components of the spin density and of the one-dimensional magnetization are also uniform. Thus the QSH quantum dot allows one to control the magnetization $M^z = -g\mu_B \rho^z / \hbar \approx \mu_B I / ev_F$ of the whole edge with a gate voltage applied locally to the dot. The conductance on resonance is $G = e^2/h$. For a bias voltage of half the maximum bulk gap,²³ $V = 20$ mV, the current on resonance is thus $I = 7.7 \times 10^{-7}$ A. The resulting magnetization is $M^z \approx 9.0 \times 10^6 \mu_B \text{ m}^{-1}$. Clearly, the magnetic moment carried by a QSH edge of a typical length¹⁰ of a few times 10^{-4} m is small and probably hard to measure in the vicinity of the ferromagnetic barriers.

A probably better approach to probing the magnetization of the QSH edge is to study the spin-filter effect of the device. Since all electrons moving to the right (left) have spin up (down), the charge current I corresponds to a magnetic-moment current of $I_\mu \approx \mu_B I / e = 4.8 \times 10^{12} \mu_B \text{ s}^{-1}$. This is the magnetic moment deposited per second in both contacts to the measurement apparatus. This suggests to measure the accumulated spin in the contacts or to study the transport through the device using ferromagnetic electrodes. In the limiting case of half-metallic ferromagnets and perfect spin injection, the measurement would only register a current for one sign of the bias voltage but not for the other.

V. SUMMARY

We have considered a quantum dot in a QSH edge realized by two thin magnetic tunneling barriers with parallel or antiparallel exchange fields. For a vanishing electron-electron interaction, arbitrary strengths of the magnetic barriers are studied within the Landauer approach. The linear dispersion of edge states leads to an equidistant ladder of dot resonances and to a double periodicity of the differential conductance in both gate and bias voltages. The features are washed out for weak barriers.

In the interacting case, we employ the Pauli master equation in a sequential-tunneling approximation including level broadening, which is valid for strong magnetic barriers. The approach also becomes exact in the two limits of vanishing barriers and of weak interaction. For increasing Coulomb interaction, the Coulomb-blockade diamonds grow,

as expected. The periodicity of the differential conductance in the gate voltage is preserved, albeit with increased period, while the periodicity in the bias voltage is destroyed. For strong interactions, the *noninteracting* period reemerges. Spin-momentum locking leads to a proportionality between the charge current, the z component of the magnetization of the whole QSH edge, and the magnetic moment deposited in the contacts to the device. This opens the possibility to control the magnetization by a locally applied gate voltage.

ACKNOWLEDGMENTS

The author would like to thank T. Ludwig, A. P. Schnyder, E. M. Hankiewicz, A. Wacker, J. König, and A. Croy for useful discussions. Financial support by the Deutsche Forschungsgemeinschaft, in part through Research Unit 1154, is gratefully acknowledged.

*carsten.timm@tu-dresden.de

¹M. Z. Hasan and C. L. Kane, *Rev. Mod. Phys.* **82**, 3045 (2010).

²S. Ryu, A. Schnyder, A. Furusaki, and A. Ludwig, *New J. Phys.* **12**, 065010 (2010).

³X.-L. Qi and S.-C. Zhang, *Rev. Mod. Phys.* **83**, 1057 (2011).

⁴A. P. Schnyder, S. Ryu, A. Furusaki, and A. W. W. Ludwig, *Phys. Rev. B* **78**, 195125 (2008); *AIP Conf. Proc.* **1134**, 10 (2009).

⁵A. Yu. Kitaev, *AIP Conf. Proc.* **1134**, 22 (2009).

⁶M. R. Zirnbauer, *J. Math. Phys.* **37**, 4986 (1996); A. Altland and M. R. Zirnbauer, *Phys. Rev. B* **55**, 1142 (1997).

⁷S. Murakami, N. Nagaosa, and S. C. Zhang, *Science* **301**, 1348 (2003); *Phys. Rev. Lett.* **93**, 156804 (2004).

⁸J. Sinova, D. Culcer, Q. Niu, N. A. Sinitsyn, T. Jungwirth, and A. H. MacDonald, *Phys. Rev. Lett.* **92**, 126603 (2004).

⁹B. A. Bernevig, T. L. Hughes, and S. C. Zhang, *Science* **314**, 1757 (2006).

¹⁰M. König, S. Wiedmann, C. Brüne, A. Roth, H. Buhmann, L. W. Molenkamp, X.-L. Qi, and S.-C. Zhang, *Science* **318**, 766 (2007).

¹¹M. König, H. Buhmann, L. W. Molenkamp, T. Hughes, C.-X. Liu, X.-L. Qi, and S.-C. Zhang, *J. Phys. Soc. Jpn.* **77**, 031007 (2008).

¹²G. Tkachov and E. M. Hankiewicz, *Phys. Rev. B* **83**, 155412 (2011).

¹³R. Landauer, *IBM J. Res. Dev.* **1**, 233 (1957); *Philos. Mag.* **21**, 863 (1970).

¹⁴C. Wu, B. A. Bernevig, and S.-C. Zhang, *Phys. Rev. Lett.* **96**, 106401 (2006).

¹⁵C. Xu and J. E. Moore, *Phys. Rev. B* **73**, 045322 (2006).

¹⁶J. C. Budich, F. Dolcini, P. Recher, and B. Trauzettel, *Phys. Rev. Lett.* **108**, 086602 (2012).

¹⁷C. L. Kane and M. P. A. Fisher, *Phys. Rev. B* **46**, R7268 (1992); **46**, 15233 (1992).

¹⁸A. Furusaki and N. Nagaosa, *Phys. Rev. B* **47**, 3827 (1993).

¹⁹C. de C. Chamon and X. G. Wen, *Phys. Rev. Lett.* **70**, 2605 (1993).

²⁰V. Meden, T. Enss, S. Andergassen, W. Metzner, and K. Schönhammer, *Phys. Rev. B* **71**, 041302(R) (2005).

²¹K. T. Law, C. Y. Seng, P. A. Lee, and T. K. Ng, *Phys. Rev. B* **81**, 041305(R) (2010).

²²J. I. Väyrynen and T. Ojanen, *Phys. Rev. Lett.* **106**, 076803 (2011).

²³J. C. Y. Teo and C. L. Kane, *Phys. Rev. B* **79**, 235321 (2009).

²⁴H. Bruus and K. Flensberg, *Many-Body Quantum Theory in Condensed Matter Physics* (Oxford University Press, Oxford, 2004).

²⁵M. Leijnse and M. R. Wegewijs, *Phys. Rev. B* **78**, 235424 (2008).

²⁶C. Timm, *Phys. Rev. B* **83**, 115416 (2011).

²⁷H. Schoeller and G. Schön, *Phys. Rev. B* **50**, 18436 (1994).

²⁸J. N. Pedersen and A. Wacker, *Phys. Rev. B* **72**, 195330 (2005).

²⁹S. Koller, M. Grifoni, M. Leijnse, and M. R. Wegewijs, *Phys. Rev. B* **82**, 235307 (2010).

³⁰J. Koch, F. von Oppen, Y. Oreg, and E. Sela, *Phys. Rev. B* **70**, 195107 (2004).

³¹C. Timm and F. Elste, *Phys. Rev. B* **73**, 235304 (2006).